

# Green Chemistry

Cutting-edge research for a greener sustainable future

[rsc.li/greenchem](https://rsc.li/greenchem)



ISSN 1463-9262

## PAPER

Zhicheng Jiang, Javier Remón, Changwei Hu, Bi Shi *et al.*  
On the development of chrome-free tanning agents:  
an advanced Trojan horse strategy using 'Al-Zr-  
oligosaccharides' produced by the depolymerization and  
oxidation of biomass



Cite this: *Green Chem.*, 2021, **23**, 2640

# On the development of chrome-free tanning agents: an advanced Trojan horse strategy using 'Al–Zr-oligosaccharides' produced by the depolymerization and oxidation of biomass

Zhicheng Jiang,<sup>a,b</sup> Mi Gao,<sup>a,b</sup> Javier Remón,<sup>id</sup> \*<sup>c</sup> Wei Ding,<sup>id</sup> <sup>d</sup> Changwei Hu<sup>id</sup> \*<sup>e</sup> and Bi Shi<sup>id</sup> \*<sup>a,b</sup>

This work addresses the manufacturing of a pioneering chrome-free tanning agent, consisting of 'Al–Zr-oligosaccharides' produced from biomass. First, a microwave-assisted  $\text{AlCl}_3\text{--H}_2\text{O}_2\text{--H}_2\text{O}$  reaction system was used for the simultaneous degradation and oxidation of hemicellulose in corncob. The obtained aqueous solution containing 'Al-oligosaccharides' was then combined with Zr to produce water-soluble 'Al–Zr-oligosaccharides'. These species behaved as a 'Trojan horse', allowing the uniform and controlled penetration of Al and Zr into the leather, avoiding their accumulation on the surface. The effects of the reaction temperature and the  $\text{AlCl}_3$  and  $\text{H}_2\text{O}_2$  concentrations used during the synthesis were systematically analyzed. Increases in the temperature and  $\text{AlCl}_3$  concentration improved the hemicellulose conversion, while the use of high  $\text{H}_2\text{O}_2$  concentrations augmented the amounts of  $\text{--CHO/--COOH}$  functionalities in the oligosaccharides, with both phenomena being paramount for the efficient formation of 'Al–Zr-oligosaccharides'. However, more severe reaction conditions led to the formation of an undesirable species, negatively influencing the tanning performance and chromaticity of the tanning agent. Given this, these parameters were optimized, and it was found that it is possible to convert up to 72 wt% of the hemicellulose present in corncob into an 'advanced Trojan horse tanning agent' contained in a colorless water solution, conducting the synthesis at 129 °C with a solvent comprising 56 mM  $\text{AlCl}_3$  and 2.6 vol%  $\text{H}_2\text{O}_2$ . The application of this solution for leather tanning provided leather with a shrinkage temperature as high as 87 °C, thus meeting the restrictive requirements of the leather industry. Therefore, these results are a landmark achievement in this field and represent a step forward to a sustainable and renewable leather industry.

Received 8th December 2020,  
Accepted 8th February 2021

DOI: 10.1039/d0gc04155f

[rsc.li/greenchem](http://rsc.li/greenchem)

## Introduction

Leather products have been widely recognized as life necessities since they are extensively used in many industrial applications, including clothing, footwear, luggage and furnishing. Leather is made up of animal skin, which structurally comprises collagen fibers connected within a three-dimensional

and hierarchical network.<sup>1,2</sup> From an industrial perspective, the conversion of animal skin into final leather products includes several steps, with tanning being one of the most critical parts of the process. In particular, leather tanning involves two crucial steps, a first efficient penetration of the tanning agent into the leather matrix and a subsequent cross-linking reaction between the immersed tanning agent and the collagen fibers in the leather. After the tanning process, the collagen fibers are dispersed and stabilized through a cross-linking reaction, which leads to a finished leathery material with excellent physicochemical properties to meet the quality requirements for commercial applications.<sup>3,4</sup>

Regarding the tanning agents used industrially, chromic salts have been widely employed due to their satisfactory tanning performance and competitive price. However, the more and more restrictive release limitation of chrome-containing hazardous wastewater and solid by-products led to the demand for sustainable, chrome-free tanning agents in the

<sup>a</sup>Department of Biomass Science and Engineering, Sichuan University, Chengdu, 610065, P. R. China. E-mail: shibi@scu.edu.cn; Fax: +86-28-85400356; Tel: +86-28-85400356

<sup>b</sup>National Engineering Research Center of Clean Technology in Leather Industry, Sichuan University, Chengdu, 610065, P. R. China

<sup>c</sup>Instituto de Carboquímica, CSIC, Zaragoza, 50018, Spain. E-mail: jremon@icb.csic.es

<sup>d</sup>China Leather and Footwear Research Institute Co. Ltd, Beijing, 100015, P. R. China

<sup>e</sup>Key Laboratory of Green Chemistry and Technology, Ministry of Education, Sichuan University, Chengdu, 610065, P. R. China. E-mail: changwei@scu.edu.cn





leather industry worldwide.<sup>5–8</sup> As such, the use of chrome-free metal tanning agents, such as aluminum and zirconium salts, is regarded as a potential industrial and sustainable alternative, accounted for by their satisfactory crosslinking ability and eco-friendly nature.<sup>9</sup> However, one of the significant drawbacks of using these salts is their excellent coordination ability with the leather surface collagen fibers during the penetration procedure. This hampers the uniform penetration of metals into the leather matrix and consequently causes an undesirable and inefficient tanning effect.<sup>10</sup> To overcome this issue, a masking agent strategy was commonly used in the past. For this strategy, metals were coordinated with a series of small ligands, including the hydroxyl and carboxyl groups, such as lactic and citric acids, which acted as masking agents to improve metal penetration.<sup>11,12</sup> However, the masking behavior of these species was not very efficient, and the tanning effect was still unsatisfactory. Therefore, the design of renewable and sustainable masking agents with an appropriate coordination ability is paramount for the industrial development and implementation of a 'chrome-free leather industry'.

Given the sustainable issues the leather industry is currently facing, a possible solution to increase its sustainability might be introducing biomass-derived products into the tanning process. Lignocellulosic biomass is an abundant and widespread source of raw materials, which has been considered an alternative to petroleum to produce energy, chemicals and materials.<sup>13,14</sup> Structurally, lignocellulosic biomass mainly consists of cellulose, hemicellulose and lignin, with the former two components being polysaccharides (glucose-based and xylose-rich, respectively) and the latter a heteropolymer containing several aromatic units.<sup>15</sup> The biomass polysaccharide content has been generally converted to platform chemicals, owing to the abundant oxygen-containing groups within this fraction. As such, this strategy is capable of connecting the biomass-based chemistry with the petroleum-based industry in a more sustainable manner. The degradation of polysaccharides into oligosaccharides is the first and one of the most important steps for the efficient utilization of carbohydrates in biomass.

With regard to biomass utilization in the leather industry, the oligosaccharides produced from biomass contain various coordinating groups with a bespoke molecular size. Therefore, they could be considered as masking agents for penetrating metal ions into the leather matrix during the tanning process. In this respect, in a previous work, we developed a 'Trojan horse strategy', wherein  $\text{AlCl}_3$  was employed to catalyze the cellulose degradation into oligosaccharides and the *in situ* generation of 'Al-oligosaccharide' complexes, which served as the tanning agent.<sup>16</sup> However, the crosslinking reaction between the Al species and collagen fibers was not strong enough. Besides, the shrinkage temperature ( $T_s$ ) of the tanned leather had to be measured in glycerol rather than in water. To overcome this issue and improve the leather quality, it is necessary to use a metal ion with a stronger coordination ability with the collagen fibers to enhance the crosslinking reactions. This also requires modifying the chemical features of these oligosaccharides to enhance their masking capabilities

to avoid the overloading of metals on the leather surface. It must also be borne in mind that when a solution with a moderate pH is used (required for the leather industry), the cellulose structure can only be softened and degraded at a reaction temperature above 180 °C,<sup>17,18</sup> which makes the application of biomass in the leather industry more challenging.

Herein, an advanced, industrially competitive, 'advanced Trojan horse strategy' has been addressed in this work to produce a carbon-neutral and environmentally friendly tanning agent. This new optimized Trojan horse approach includes two steps. The first part comprises the simultaneous 'one-pot' degradation and oxidation of hemicellulose in corncob, a typical unavoidable food waste produced worldwide, using an  $\text{AlCl}_3\text{-H}_2\text{O}_2$  solution at a relatively low temperature, for the formation of a high-efficient and sustainable tanning carrier, *i.e.*, 'the horse'. The second step includes the addition of Zr and more Al species to produce an 'advanced Trojan horse' tanning agent. This advanced tanning agent consists of an aqueous solution containing 'Al-Zr-oligosaccharide' complexes, with excellent tanning properties to meet the quality standards of the leather industry. For this, the effects of the reaction temperature (100–160 °C), and the concentrations of  $\text{AlCl}_3$  (0.01–0.1 mM) and  $\text{H}_2\text{O}_2$  (1–5 vol%) and all possible interactions between these factors were thoroughly investigated on the production of our advanced and sustainable 'advanced Trojan horse' tanning agent, carefully evaluating its performance in the tanning of pickled cattle pelt. As such, this work represents a step forward for the transition from an unsustainable and hazardous leather industry to an industrially competitive, chrome-free, sustainable, carbon-neutral and efficient leather industry.

## Results and discussion

The results corresponding to the synthesis of the tanning agent and its tanning behavior are listed in Table 1. The relative influence of the operating variables on the results according to the ANOVA and the cause-effect Pareto principle are listed in Table 2.

### Conversion of the hemicellulose, cellulose and lignin fractions in corncob

The hemicellulose conversion varied from 37 to 95%. The lignin and cellulose conversion shifted by 1–34% and 9–23%, respectively, thus indicating that the  $\text{AlCl}_3\text{-H}_2\text{O}_2$  system used in the synthesis step is very efficient for the selective conversion of hemicellulose in corncob. Regarding the relative influence of the synthesis parameters, the cause-effect Pareto analysis reveals that the reaction temperature exerts the most important influence on hemicellulose conversion, followed by the  $\text{AlCl}_3$  concentration (45 and 17% of the influence, respectively). Furthermore, the interactions between these two variables also exert a significant influence (15%). To explain the effects of the synthesis conditions and the interactions between them on the conversion of hemicellulose, cellulose and lignin, 3D surface plots were developed from the ANOVA



**Table 1** Influence of the synthesis conditions on the preparation and performance of the tanning agent

Run	1	2	3	4	5	6	7	8	9–12		13	14	15	16	17	18
Temperature (°C)	100	160	100	160	100	160	100	160	130		100	160	130	130	130	130
AlCl <sub>3</sub> concentration (mM)	10	10	100	100	10	10	100	100	55		55	55	10	100	55	55
H <sub>2</sub> O <sub>2</sub> concentration (vol%)	1	1	1	1	5	5	5	5	3		3	3	3	3	1	5
Biomass conversion results																
Hemicellulose conversion (%)	37.7	77.8	46.0	93.1	46.6	86.9	60.9	94.5	74.9 ± 1.9		41.3	90.7	52.9	79.6	58.4	81.9
Cellulose conversion (%)	9.6	11.0	8.9	20.7	17.1	22.6	18.4	23.0	15.7 ± 1.0		15.1	22.9	16.9	20.4	11.6	22.7
Lignin conversion (%)	1.2	22.8	4.6	29.2	24.3	32.7	21.7	33.5	24.5 ± 2.8		11.4	32.6	20.8	31.4	18.1	32.5
Properties of the hydrolysate																
Colorimetry of the hydrolysate (a.u.)	272	3036	491	6493	450	3751	1473	9782	4812.3 ± 113.2		643	6930	2320	5043	2717	5589
Monosaccharide yield (wt%)	0.2	12.9	0.4	11.0	0.5	14.3	1.6	10.1	5.9 ± 0.2		0.6	13.7	1.3	7.5	1.9	9.8
Acid yield (wt%)	1.1	3.0	1.6	5.1	5.8	8.1	7.3	9.0	5.3 ± 0.3		5.0	6.9	4.7	4.8	2.0	7.7
Furan yield (wt%)	0.0	0.7	0.0	4.8	0.0	0.4	0.0	4.7	0.1 ± 0.0		0.0	3.0	0.0	0.2	0.0	0.2
Evaluation of the tanning performance																
Shrinkage temperature (°C)	74.4	84.1	79.0	85.5	80.6	86.1	80.4	86.0	87.7 ± 0.6		78.5	87.0	82.0	85.9	81.0	90.6
Al absorption (wt%)	79.5	77.8	85.3	85.1	75.7	60.9	74.2	76.7	75.0 ± 0.9		74.8	74.1	64.3	69.0	77.4	82.7
Zr absorption (wt%)	93.3	94.4	85.9	88.7	90.8	74.1	86.5	88.7	88.6 ± 0.8		93.5	90.0	76.5	82.0	93.4	91.4

**Table 2** Relative influence of the operating conditions according to the ANOVA

Variable	R <sup>2</sup>	Term	Indep.														
			A T	B AlCl <sub>3</sub>	C H <sub>2</sub> O <sub>2</sub>	AB	AC	BC	ABC	A <sup>2</sup>	B <sup>2</sup>	C <sup>2</sup>	A <sup>2</sup> B	A <sup>2</sup> C	AB <sup>2</sup>	A <sup>2</sup> B <sup>2</sup>	
Biomass conversion results																	
Hemicellulose conversion (%)	0.99	74.9	24.7 (40)	13.4 (14)	11.8 (11)		−1.7 (3)		−1.7 (3)	−8.9 (5)	−8.6 (3)	−4.7 (1)	−7.7 (6)	−7.5 (5)	−4.6 (3)	15.2 (6)	
Cellulose conversion (%)	0.96	16.2	3.11 (23)	1.42 (11)	4.2 (31)	1.2 (8)		−0.9 (6)	−1.4 (9)	2.8 (1)	2.5 (1)					−5.1 (10)	
Lignin conversion (%)	0.97	25.1	8.8 (34)	5.3 (7)	6.9 (27)		−3.3 (11)	−1.5 (5)		−3.7 (10)			−4.3 (6)				
Properties of the hydrolysate																	
Hydrolysate chromaticity (a.u.)	0.99	4812.	3143 (31)	1345 (16)	1436 (9)	1030 (11)	355 (4)	422 (4)	221 (2)	−1025 (8)	−1130 (5)	−659 (1)		−790 (4)	−596 (3)	1222 (2)	
Monosaccharide yield (wt%)	0.99	5.85	6.6 (44)	3.1 (1)	4.0 (7)	−0.9 (6)	−0.1 (1)	−0.2 (1)	−0.4 (3)	1.3 (5)	−1.5 (5)		−3.7 (11)	−3.7 (11)	−0.9 (3)	0.7 (2)	
Acid yield (wt%)	0.99	5.3	1.1 (21)		2.9 (46)		−0.2 (3)		−0.3 (4)	0.7 (3)	−0.5 (5)	−0.4 (6)	0.6 (10)	−0.4 (2)			
Furan yield (wt%)	0.99	0.1	1.5 (29)	0.1 (18)	0.1 (1)	1.1 (20)	−0.1 (1)			1.4 (19)			1.0 (9)	−0.2 (1)	−0.2 (1)	−0.2 (1)	
Evaluation of the tanning performance																	
Shrinkage temperature (°C)	0.97	87.6	3.6 (27)	1.0 (7)	4.8 (15)			−0.8 (5)		−4.9 (20)	−3.7 (8)	−1.9 (0)		−3.5 (11)		4.8 (7)	
Al absorption (wt%)	0.99	74.8		2.2 (10)	2.6 (12)	1.1 (5)		1.4 (6)	3.2 (13)		−8.1 (7)	5.3 (18)		−6.4 (12)	−3.0 (12)	3.7 (5)	
Zr absorption (wt%)	0.99	88.3	−1.4 (7)	2.7 (1)		2.6 (10)	−2.3 (9)	2.9 (12)	2.1 (9)	3.7 (4)	−8.7 (19)	4.4 (11)	−3.1 (6)	−2.8 (12)			

Response = indep. term + coefficient  $A \cdot A$  + coefficient  $B \cdot B$  + coefficient  $C \cdot C$  + coefficient  $AB \cdot AB$  + coefficient  $AC \cdot AC$  + coefficient  $BC \cdot BC$  + coefficient  $ABC \cdot ABC$  + coefficient  $A^2 \cdot A^2$  + coefficient  $B^2 \cdot B^2$  + coefficient  $C^2 \cdot C^2$  + coefficient  $A^2B \cdot A^2B$  + coefficient  $A^2C \cdot A^2C$  + coefficient  $AB^2 \cdot AB^2$  + coefficient  $A^2B^2 \cdot A^2B^2$ . Numbers in brackets indicate the percentage Pareto influence of each factor on the response variable. Pareto values represent the percentage of the orthogonal estimated total value.

of the results (Table 2). Fig. 1 shows the effects of the reaction temperature and H<sub>2</sub>O<sub>2</sub> concentration on the conversion of hemicellulose, cellulose and lignin in corncob with different AlCl<sub>3</sub> concentrations.

The effects of the synthesis temperature and concentration of H<sub>2</sub>O<sub>2</sub> depend on the concentration of AlCl<sub>3</sub>. For a diluted AlCl<sub>3</sub> (10 mM) solution, the conversion of hemicellulose depends on the temperature. While at low temperatures

(100–130 °C), the hemicellulose conversion is as low as 50%, and an increase in the reaction temperature up to 160 °C leads to a sharp rise in the hemicellulose conversion, due to the positive kinetic effect of the temperature on hemicellulose depolymerization. Increasing the concentration of AlCl<sub>3</sub> modifies the impact of the temperature. In particular, when the AlCl<sub>3</sub> concentration is increased progressively from 10 to 100 mM, the hemicellulose conversion upsurges between 100



and 130 °C and remains steady with further temperature increment. Besides, the greater the concentration of  $\text{AlCl}_3$  in the mixture, the lower the temperature required to achieve an almost complete hemicellulose conversion (>90%) due to the positive effect of  $\text{AlCl}_3$  on hemicellulose depolymerization. Besides, the impact of the  $\text{H}_2\text{O}_2$  concentration on the hemicellulose conversion is less critical and depends on the temperature. This reveals that only the reaction temperature and the acidity of the reaction medium (achieved with  $\text{AlCl}_3$ ) are responsible for the cleavage of the glycosidic bonds in corncob to obtain the dissolved oligosaccharides. The efficient degradation of hemicellulose catalyzed by  $\text{AlCl}_3$  takes place following a cascade mechanism. Firstly,  $\text{AlCl}_3$  partly hydrolyzes in the aqueous solution, releasing  $\text{H}^+$  and  $\text{Cl}^-$  into the reaction system. Thus,  $\text{AlCl}_3$ , like the Lewis and Brønsted acids, breaks the glycosidic bonds in hemicellulose.<sup>19,20</sup> Secondly, the  $\text{Cl}^-$  species help destroy the hydrogen network in hemicellulose by generating hydrogen bonds with the  $-\text{OH}$  functionalities present in this carbohydrate.<sup>21</sup> Finally, once hemicellulose has been degraded into oligosaccharides, these species are further oxidized by  $\text{H}_2\text{O}_2$ . The C–C bond between C2 and C3 could be cleaved, generating two  $-\text{COOH}$  groups *via* this oxidation process.<sup>22,23</sup>

Regarding the conversion of cellulose in corncob, the reaction temperature and  $\text{H}_2\text{O}_2$  concentration contribute with an influence of 24% and 31%, respectively, whereas the  $\text{AlCl}_3$  concentration has a less significant influence (12%). Under mild reaction conditions (1 vol% of  $\text{H}_2\text{O}_2$  and 10 mM  $\text{AlCl}_3$ ), the effect of the temperature on the cellulose conversion is meager, and a steady conversion occurs between 100 and

160 °C. In contrast, an increase in the cellulose conversion is observed when higher concentrations of  $\text{AlCl}_3$  or  $\text{H}_2\text{O}_2$  are used. This is in good agreement with the literature, as the cellulose structure can only be softened at temperatures above 180 °C by hydrothermal treatment.<sup>17,18</sup> At the same time, this transition can be strengthened to some extent at lower temperatures with the use of concentrated  $\text{AlCl}_3$  or  $\text{H}_2\text{O}_2$  solutions. Besides, the influence of the concentration of  $\text{AlCl}_3$  relies on the  $\text{H}_2\text{O}_2$  concentration and temperature. On the one side, for a low  $\text{H}_2\text{O}_2$  concentration, an increase in the concentration of  $\text{AlCl}_3$  between 10 and 55 mM increases the cellulose conversion. In contrast, further increment up to 100 mM only produces a significant effect at low temperatures. On the other side, for a high  $\text{H}_2\text{O}_2$  concentration, the impact of the  $\text{AlCl}_3$  concentration is meager.

These differences might be accounted for by a different depolymerization mechanism occurring in the presence of  $\text{H}_2\text{O}_2$ . In this case, the rupture of the hydrogen bonding networks between the glucose chains in the cellulose occurs *via* a first  $\text{H}_2\text{O}_2$  oxidation of the hydroxyl groups of the cellulose outer layer, followed by subsequent depolymerization occurring layer-by-layer.<sup>24,25</sup> To gain more insights into these phenomena, the crystalline index (CI) of cellulose was determined (by XRD) after the catalytic treatment. This allows evaluating the damage of the crystalline cellulose region in corncob (Fig. 2). Due to the efficient removal of the hemicellulose fraction and part of the lignin and cellulose, the crystal structure of the solid fraction became neater and had an elevated CI. However, the CI of this solid residue was reduced with a further increase in the reaction temperature and/or by using a

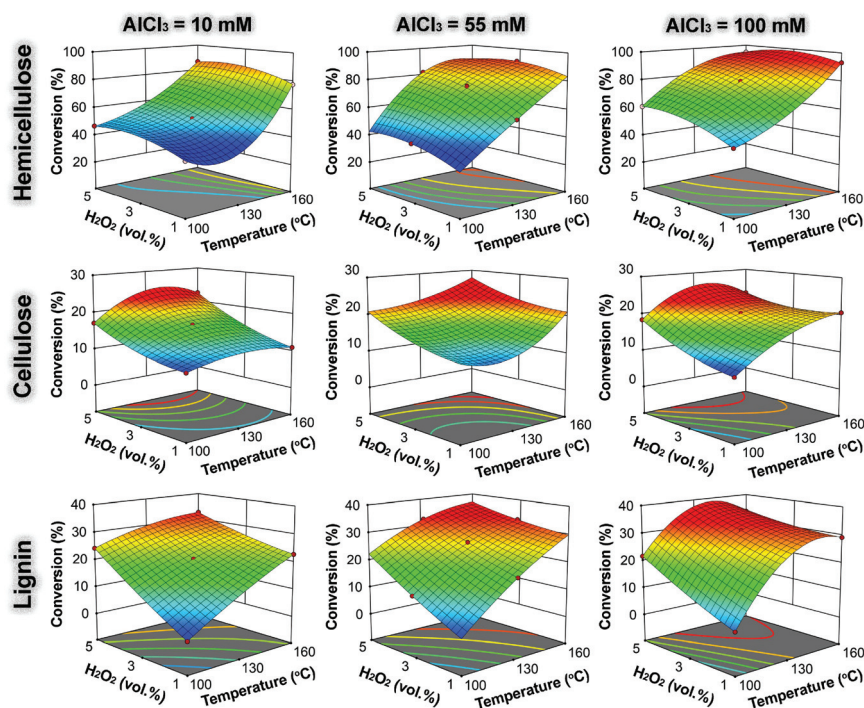


Fig. 1 3D surface plots of the reaction temperature and  $\text{H}_2\text{O}_2$  concentration with different  $\text{AlCl}_3$  concentrations for the conversion of hemicellulose, cellulose and lignin in corncob.



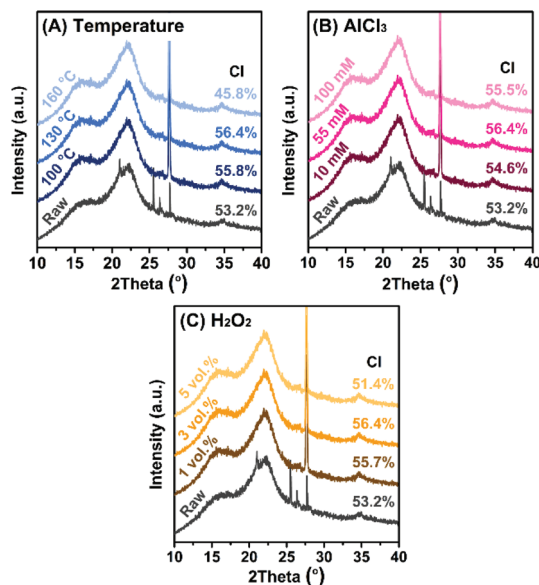


Fig. 2 XRD patterns and the relative crystalline index (CI) of corncob and the reaction residues obtained at different (A) Temperatures, (B)  $\text{AlCl}_3$  concentrations and (C)  $\text{H}_2\text{O}_2$  concentrations.

higher  $\text{H}_2\text{O}_2$  concentration, providing evidence for the dominant effect of these two operating variables on the cellulose conversion.

The reaction temperature and  $\text{H}_2\text{O}_2$  concentration primarily influence the conversion of lignin. To achieve a high lignin conversion, both degradation and solubilization of this structural component must take place simultaneously, *i.e.*, the reaction medium must behave dually. On the one hand, it must ensure a nucleophilic performance to break down the lignin network into fragments; on the other, it must act as an electron donor organic solvent with middle polarity to dissolve the liberated fragments with low hydrophilicity.<sup>26–28</sup> Given this, the organic solvent-free reaction system used in this work is incapable of dissolving the macromolecular lignin oligomers. Therefore, the reaction temperature is responsible for the degradation of the easily converted part of lignin, thus explaining the increase in the lignin conversion with increasing the reaction temperature. At the same time, an increase in the  $\text{H}_2\text{O}_2$  concentration helps improve the hydrophilicity of the degraded lignin oligomers *via* oxidation, which increases the lignin conversion when the concentration of  $\text{H}_2\text{O}_2$  is increased from 1 to 5 vol%.

### Presence of low molecular weight products in the tanning liquid (hydrolysate)

The chemical analysis of the hydrolysate reveals that the converted corncob solubilized in the liquid (hydrolysate) primarily consisting of a mixture of oligomers, including principally oxidized xylo-oligomers, derived from the depolymerization/oxidation of hemicellulose.

Besides, ligno-oligomers and cello-oligomers, produced from the side decomposition of part of the lignin and cellulose fractions, respectively, are also present in the liquid effluent to

a lesser extent.<sup>29</sup> Apart from these macromolecules, the hydrolysate also contains small amounts of low molecular weight products yielded from the hydrolysis and decomposition of these oligomers. These species include monosaccharides (mainly xylose and glucose), carboxylic acids (primarily formic and acetic acids) and furans (5-HMF and furfural).

As the active biomass species in the ‘advanced Trojan horse’ tanning agent are oxidized xylo-oligomers, it is paramount to detect, analyze and minimize the yields of these small molecular products. The presence of these chemicals not only decreases the availability of oxidized xylo-oligosaccharides in the tanning agent, but also could hamper the tanning process. Notably, they might negatively impact the chromaticity of the liquid solution and, therefore, the tanned leather, thus impeding its commercial use. The yields of monosaccharides, carboxylic acids and furans varied from 0 to 14 wt%, from 1 to 9 wt%, and from 0 to 5 wt%, respectively. Regarding the influence of the processing conditions, the Pareto test reveals that the yields of monosaccharides and furans are primarily affected by the reaction temperature (around 50% of the influence). In comparison, the yield of carboxylic acids depends mostly on the  $\text{H}_2\text{O}_2$  concentration (52% of the influence). To understand these effects, Fig. 3 shows the influence of the temperature on the yields of monosaccharides, carboxylic acids and furans for the different amounts of  $\text{AlCl}_3$  and  $\text{H}_2\text{O}_2$  used in the synthesis step.

Regardless of the  $\text{AlCl}_3$  or  $\text{H}_2\text{O}_2$  concentrations, an increase in the synthesis temperature from 100 to 160 °C leads to increases in the proportions of monosaccharides, carboxylic acids and furans, resulted from a higher conversion of corncob and the following decomposition reactions. Besides, the effect of the temperature also relies on the  $\text{AlCl}_3$  and  $\text{H}_2\text{O}_2$  concentrations. In particular, the impact of the temperature on the monosaccharide and furan yields depends on the concentration of  $\text{AlCl}_3$ . Irrespective of the  $\text{H}_2\text{O}_2$  concentration, when a low amount of this salt is used, the yield of furans is meager, and the formation of monosaccharides is only significant at temperatures higher than 130 °C. Besides, an increase in the  $\text{AlCl}_3$  concentration increases the yields of monosaccharides (between 110 and 145 °C) and furans (between 130 and 160 °C). These increase the result from the kinetic effect of  $\text{AlCl}_3$  on both, the first hydrolysis of oligosaccharides into monosaccharides, and the subsequent decomposition of these species into furans when high temperatures are used.

The impact of the concentration of  $\text{H}_2\text{O}_2$  on the yields of monosaccharides and furans is relatively weak, especially for the former species. In general, an increase in the concentration of  $\text{H}_2\text{O}_2$  from 1 to 5 vol% increases the monosaccharide yield between 100 and 140 °C when high  $\text{AlCl}_3$  (100 mM) concentrations are used. This might be accounted for by the looser structures of the polysaccharides with broken hydrogen bonding networks due to  $\text{H}_2\text{O}_2$  oxidation. Therefore, the combination of high  $\text{H}_2\text{O}_2$  and  $\text{AlCl}_3$  concentrations increases the presence of monosaccharides at low temperatures. At a high temperature, a trend-off is observed for the proportion of these species, which suggests their transformation into secondary





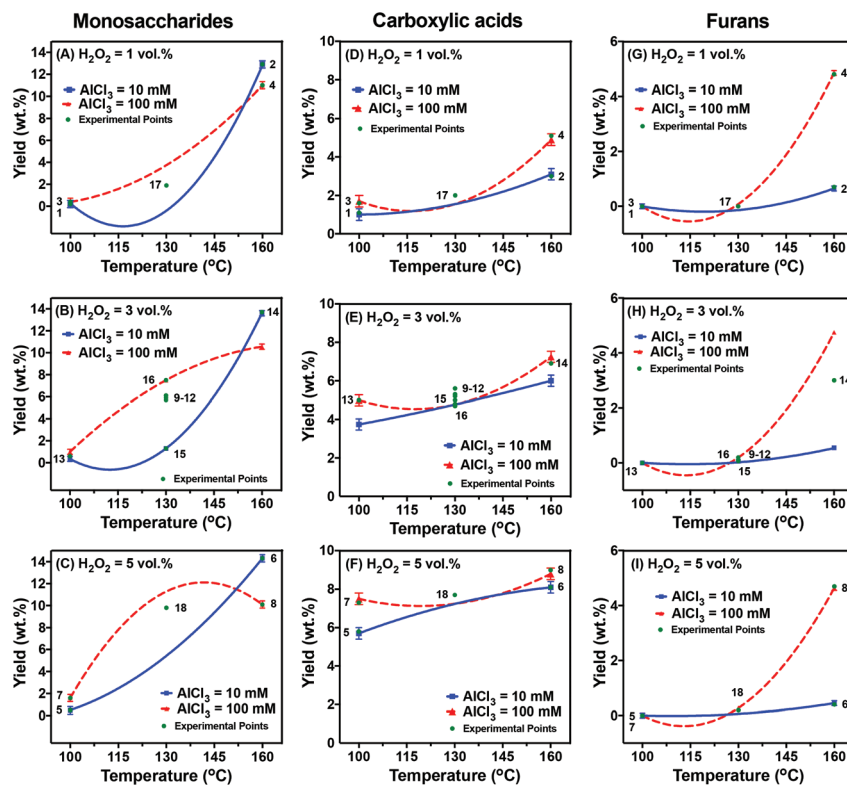


Fig. 3 Interaction plots for the yields of (A–C) monosaccharides, (D–F) carboxylic acids and (G–I) furans.

products, mainly furans. In contrast, the proportion of  $\text{H}_2\text{O}_2$  exerts a significant influence on the concentration of carboxylic acids, and an increase from 1 to 5 wt% substantially increases the proportion of these acids in the liquid. This can be explained by the production of more carboxylic acids as part of the oxidation process.

#### Chromaticity of the liquid phase (hydrolysate) used for the development of the advanced Trojan horse tanning agent

The liquid effluent resulting from the catalytic conversion of hemicellulose in corncob, containing the  $\text{Al}^{3+}$  species together with oxidized oligosaccharides, was used to synthesize 'Al-Zr-oligosaccharide' water solutions. As commented above, this aqueous liquid could also include other species resulting from the side reactions, which may alter the color of this effluent. As this circumstance hampers the commercial application of the prepared leather, the chromaticity (arbitrary units, AU) of the hydrolysate produced during the synthesis step was measured and analyzed.

As shown in Fig. 4, depending on the synthesis conditions, the color of the liquid tanning agent precursor varies from light yellow to dark brown, resulting in a chromaticity variation between 272 and 9782, respectively. Specifically, at 100 °C, a light to yellow liquid with a chromaticity lower than 1500 is attained regardless of the  $\text{AlCl}_3$  and  $\text{H}_2\text{O}_2$  dosages. In contrast, a chromaticity higher than 4000 and a red to brown tanning liquid precursor is observed at 160 °C. This is in accordance with the fact that the reaction temperature exerts

the most significant impact, with 39% influence, on the chromaticity of the solution. Simultaneously, the  $\text{AlCl}_3$  and  $\text{H}_2\text{O}_2$  concentrations also significantly affect the liquid chromaticity, with 21% and 10% influence, respectively. Thus, the chromaticity of the tanning agent increases along the bottom-left to the top-right (higher  $\text{AlCl}_3$  and  $\text{H}_2\text{O}_2$  concentrations) in the  $\text{AlCl}_3$ – $\text{H}_2\text{O}_2$  two-dimensional correlation (Fig. 4B and C). Higher reaction temperatures promote not only the degradation of corncob, but also the production of more free radical fragments.  $\text{AlCl}_3$ , like both Lewis and Brønsted acids, endorses the former process, whereas  $\text{H}_2\text{O}_2$  promotes the latter route. Meanwhile, the radical repolymerization can also be accelerated in this acidic reaction environment, and the colored oligomers, such as 'oligosaccharide-furan' complexes and 'oligosaccharide-ligno-oligomers', can be consequently generated.<sup>29</sup>

#### Influence of the synthesis conditions on the tanning performance of the 'advanced Trojan horse' tanning agent

Prior to the tanning process, additional  $\text{AlCl}_3 \cdot 6\text{H}_2\text{O}$  (totally equal to 2 wt% of  $\text{Al}_2\text{O}_3$ ) along with  $\text{Zr}(\text{SO}_4)_2 \cdot 4\text{H}_2\text{O}$  (equal to 6 wt% of  $\text{ZrO}_2$ ) were added to the hydrolysate as the final step for the preparation of the 'advanced Trojan horse' tanning agent. Its performance was evaluated in the tanning of pickled cattle skin. For this, the shrinkage temperature ( $T_s$ ) of the tanned leather and the amounts of Al and Zr absorbed on the leather were correlated to the conditions (temperature and  $\text{AlCl}_3$  and  $\text{H}_2\text{O}_2$  concentrations) used in the synthesis step.



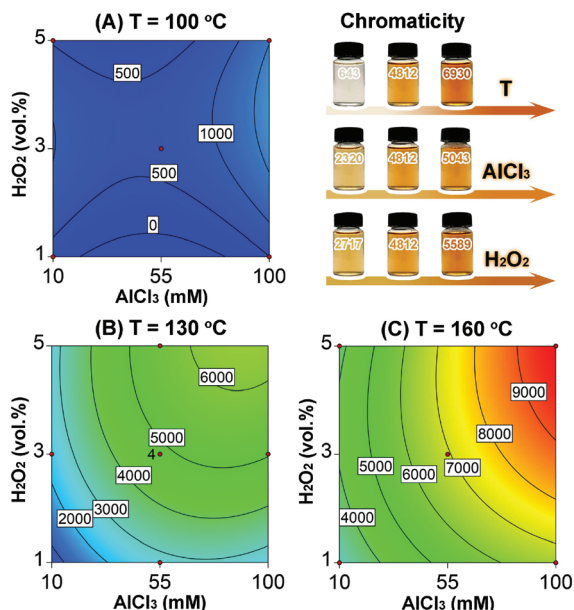


Fig. 4 Images of the reaction fluids and the contour plots for the chromaticity of the reaction fluids:  $T = 100\text{ }^{\circ}\text{C}$  (A),  $T = 130\text{ }^{\circ}\text{C}$  (B) and  $T = 160\text{ }^{\circ}\text{C}$  (C).

According to the cause-effect Pareto analysis (Table 2), the  $T_s$  of the tanned leather is highly influenced (47%) by the reaction temperature used in the hydrothermal synthesis reaction. Besides, the  $\text{AlCl}_3$  and  $\text{H}_2\text{O}_2$  concentrations also exert an equally (15%) significant importance. The effects of the temperature and  $\text{AlCl}_3$  concentration for a  $\text{H}_2\text{O}_2$  concentration of 1/3/5 vol% are graphically represented in Fig. 5 using 3D plots.

These representations reveal that the  $T_s$  of the tanned leather depends on the catalytic temperature used in the synthesis step. At a low temperature ( $100\text{ }^{\circ}\text{C}$ ), regardless of the  $\text{AlCl}_3$  and  $\text{H}_2\text{O}_2$  concentrations, the temperature of the tanned leather  $T_s$  is lower than  $80\text{ }^{\circ}\text{C}$ . However, an increase in the

temperature leads to an enhancement in the  $T_s$  up to around  $90\text{ }^{\circ}\text{C}$ , thus making this product appropriate to meet the restrictive requirements for commercial application. Such an enhancement in the  $T_s$  of the tanned leather goes in line with the increases observed for the hemicellulose conversion when the hydrothermal synthesis temperature increases. Thus, this development helps to provide evidence for the core effect of the xylo-oligosaccharide concentration on the tanning performance of our 'advanced Trojan horse' tanning agent.

Besides, the specific impact of the hydrothermal synthesis temperature on the  $T_s$  of the tanned leather depends on the concentrations of  $\text{H}_2\text{O}_2$  and  $\text{AlCl}_3$ . The  $\text{H}_2\text{O}_2$  concentration is a decisive factor affecting the  $T_s$  of the tanned leather, as the oxidation process can introduce  $-\text{CHO}$  and  $-\text{COOH}$  functionalities into the oligosaccharide structure.<sup>9</sup> These functionalities aid in improving the coordination ability of the oligosaccharides and consequently promote their masking performance (Trojan horse effect), thus increasing the penetration efficiency of Al and Zr ions into the leather matrix. As such, regardless of the temperature or  $\text{AlCl}_3$  concentration, the contour profiles show that an increase in the  $\text{H}_2\text{O}_2$  concentration between 1 and 5 vol% leads to a substantial increase in the  $T_s$  from  $74\text{--}84\text{ }^{\circ}\text{C}$  to  $82\text{--}90\text{ }^{\circ}\text{C}$ . Besides, the best tanning performance takes place using  $\text{H}_2\text{O}_2$  concentrations between 3 and 5 vol%, along with hydrothermal synthesis temperatures higher than  $130\text{ }^{\circ}\text{C}$ . Under such synthesis conditions, oligosaccharides (mostly xylo-oligosaccharides) with moderate  $-\text{CHO}/-\text{COOH}$  contents are produced. As a result, the oligosaccharides have a satisfactory masking effect, thus resulting in a tanned leather product with a very high  $T_s$  ( $>82\text{ }^{\circ}\text{C}$ ). With regard to the impact of the concentration of  $\text{AlCl}_3$ , the contour profiles in Fig. 5 reveal that its influence depends on the temperature and, to a greater extent, on the  $\text{H}_2\text{O}_2$  concentration. In particular, the effect of the concentration of this species is at its greatest at intermediate temperatures ( $120\text{--}140\text{ }^{\circ}\text{C}$ ) using  $\text{H}_2\text{O}_2$  concentrations ranging between 3 and 5 vol%. This seems to indicate

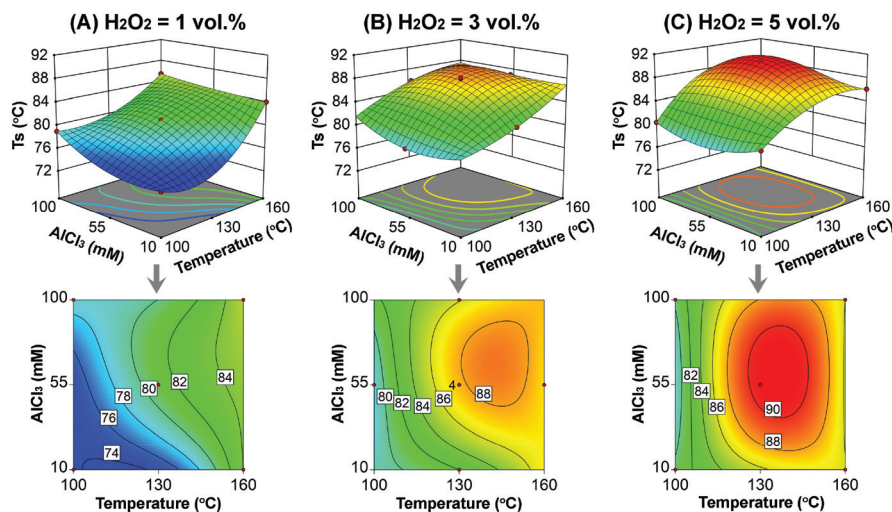


Fig. 5 3D surface plots and contour plots of the reaction temperature and  $\text{AlCl}_3$  concentration with different  $\text{H}_2\text{O}_2$  concentrations (1 vol% (A), 3 vol% (B) and 5 vol% (C)) for the shrinkage temperature of the leather tanned by the corresponding reaction fluid together with  $\text{Zr}(\text{SO}_4)_2 \cdot 4\text{H}_2\text{O}$ .





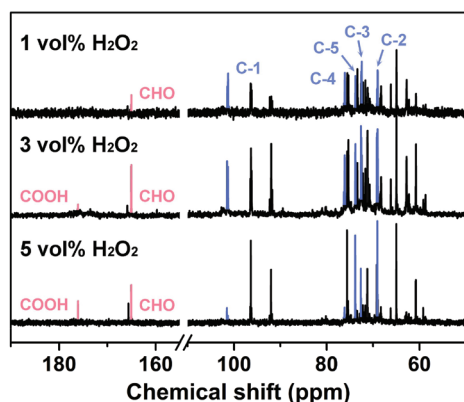


Fig. 6  $^{13}\text{C}$  NMR spectra of the reaction fractions with 55 mM  $\text{AlCl}_3$  and different  $\text{H}_2\text{O}_2$  concentrations at 130 °C.

that a moderate concentration of the oxidized oligosaccharides with abundant  $-\text{CHO}/-\text{COOH}$  is beneficial for the performance of the ‘advanced Trojan horse’ tanning agent.

To provide evidence for these phenomena, the tanning agent produced from the hydrolysate obtained at 130 °C using 55 mM  $\text{AlCl}_3$ , and different  $\text{H}_2\text{O}_2$  concentrations were analyzed by NMR (Fig. 6). All NMR signals corresponding to the xylose skeleton are observed, while the signals attributed to the presence of lignin are not detected. This demonstrates that the tanning agent synthesized consists of high purity oligosaccharides. Besides,  $-\text{CHO}$  species are only generated when a diluted (1 vol%)  $\text{H}_2\text{O}_2$  solution is used. In contrast,  $-\text{CHO}$  and  $-\text{COOH}$  species are produced using greater  $\text{H}_2\text{O}_2$  concentrations. These differences are in excellent agreement with the positive effect of the  $\text{H}_2\text{O}_2$  concentration on the tanned leather  $T_s$ . Al and Zr are coordinated with the  $-\text{COOH}$  functionalities present in the oligosaccharides. Therefore, the mechanism of our advanced ‘Al–Zr-oligosaccharide’ tanning agent involves a two-step ‘Trojan horse’ strategy. Firstly, ‘Al–Zr-oligosaccharides’ complexes penetrate the leather matrix. Before penetration, Al and Zr are coordinated with the  $-\text{COOH}$  functionalities present in the oligosaccharides. Once inside, Al and Zr ions are released from the complex and coordinate with the  $-\text{COOH}$  functionalities of the collagen fibers. In this step, an efficient cross-linking reaction takes place, which disperses and stabilizes the leather collagen fibers.

#### Influence on the amounts of Al and Zr absorbed on the leather

The cause–effect Pareto analysis (Table 2) reveals that the amounts of Al and Zr absorbed on the leather strongly depends on both the  $\text{AlCl}_3$  and  $\text{H}_2\text{O}_2$  concentrations used in the synthesis step. In contrast, the effect of the synthesis temperature is less critical. However, the relative influence of the concentrations of  $\text{AlCl}_3$  and  $\text{H}_2\text{O}_2$  on the adsorptions of Al and Zr on the tanned leather depends on the temperature (Fig. 7). At a low temperature (100 °C), the concentration of  $\text{AlCl}_3$  does not substantially influence the adsorption of Al regardless of the  $\text{H}_2\text{O}_2$  concentration. In contrast, the adsorption of Zr increases with augmenting the concentration of  $\text{AlCl}_3$  from 10 to 55 mM, and decreases thereafter. Simultaneously, the

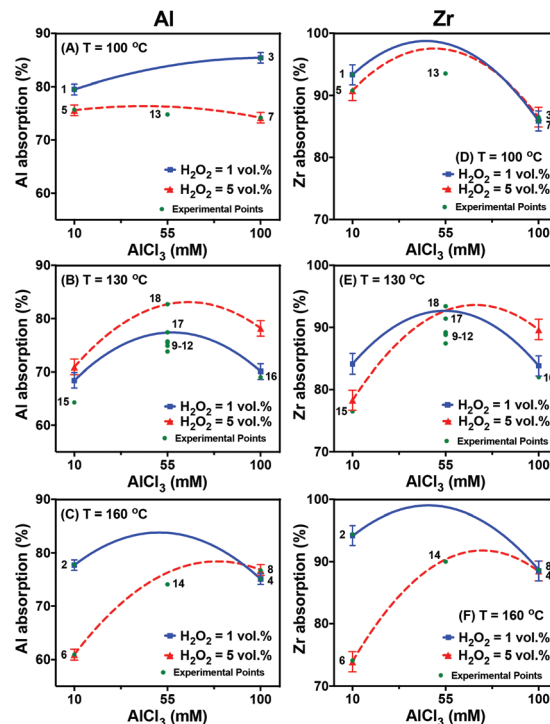


Fig. 7 Interaction plots showing the effects of the  $\text{AlCl}_3$  and  $\text{H}_2\text{O}_2$  concentrations on the Al/Zr absorptions during leather tanning at different synthesis temperatures: 100 °C (A and D), 130 °C (B and E) and 160 °C (C and F).

adsorption of Zr is not substantially affected by the amount of  $\text{H}_2\text{O}_2$  used in the synthesis step.

An increase in the reaction temperature modifies the effect of the  $\text{AlCl}_3$  and  $\text{H}_2\text{O}_2$  concentrations on the absorption of Al and Zr. At 130 °C, regardless of the  $\text{H}_2\text{O}_2$  concentration, an increase in the relative amount of  $\text{AlCl}_3$  used in the synthesis step from 10 to 55 mM leads to a substantial increase in the amounts of Al and Zr absorbed on the tanned leather. In contrast, a further increase up to 100 mM reduces the amounts of these species absorbed on the leather. At the same time, at this synthesis temperature, an increase in the concentration of  $\text{H}_2\text{O}_2$  increases the amount of Al absorbed on the leather, irrespective of the concentration of  $\text{AlCl}_3$ . In contrast, the proportion of Zr absorbed decreases with the use of  $\text{H}_2\text{O}_2$  concentrations between 10 and 55 mM and increases when the  $\text{H}_2\text{O}_2$  ranges between 55 and 100 mM.

A further increase in the temperature up to 160 °C leads to different outcomes for the amounts of Al and Zr absorbed on the leather, depending on the concentrations of  $\text{H}_2\text{O}_2$  and  $\text{AlCl}_3$  used in the synthesis step. When a low concentration of  $\text{H}_2\text{O}_2$  is used, the absorptions of Al and Zr are very high and are not highly influenced by the amounts of  $\text{AlCl}_3$ . Contrarily, increasing the amount of  $\text{H}_2\text{O}_2$  decreases the amounts of Al and Zr absorbed on the leather when  $\text{AlCl}_3$  concentrations lower than 55 mM are used. As a result, when a concentration of 5 vol% of  $\text{H}_2\text{O}_2$  is used, the amounts of Al and Zr absorbed on the leather increase with augmenting the proportion of  $\text{AlCl}_3$  in the synthesis step.



On understanding of the masking performance of the oligosaccharides to effectively introduce Al and Zr into the leather matrix, it should be noticed that there is no direct correlation between the relative amounts of Al and Zr adsorbed and the  $T_s$  of the tanning leather. This is the result of two different phenomena. On the one hand, the relative amounts of Al and Zr adsorbed were determined by the amounts of these species in the liquid effluent before and after the tanning process. Thus, this calculation considers the amounts of both these species that effectively penetrated the leather matrix and those deposited onto the leather surface. On the other, depending on the synthesis conditions, oligosaccharides with different oxidation degrees were produced, which alter the capability of these species to coordinate with Al and Zr effectively. To provide evidence for the masking and tanning effects of the 'Al-Zr-oligosaccharide' complexes, the tanned leather was characterized by stereomicroscopy and scanning electron microscopy (SEM), and the results are shown in Fig. 8.

As described above, the efficiency of the tanning agent strongly depends on the concentration of  $H_2O_2$  used in the synthesis step. When a concentration of 1 vol%  $H_2O_2$  is used, corn-like D-periodicity structures of around 65 nm with well-defined borders are observed in the tanned leather. Besides, the collagen nanofibers with an average diameter between 50 and 200 nm merge to form collagen microfibrils of ca. 2–10  $\mu m$ , fiber bundles, ranging from 20 to 100  $\mu m$ , to finally compose a 3D fibrous network.<sup>30</sup> However, stacked collagen fibers with a low dispersion degree in the tanned leather cross-section are observed, which indicate an ineffective tanning effect of 'Al-Zr-oligosaccharides'. This development can be confirmed by looking at the Al/Zr distributions on the cross-section, wherein intensive Al/Zr signals are observed on the grain and flesh layers. This phenomenon, along with the coarse and wrinkled grain surface, indicates that Al and Zr species accumulate onto the leather surface without achieving an efficient penetration (Trojan horse masking effect) into the leather matrix. This provides evidence for the low  $T_s$  of the tanned leather despite the substantial amounts of Al and Zr absorbed. A subsequent

increase in the concentration of  $H_2O_2$  up to 5 vol% during the synthesis step produces a tanned leather with smoother grains and clearer pores. At the same time, the collagen fibers display a more hierarchical dispersion, while the distributions of Al and Zr on the cross-section of the leather are more uniform. These results indicate a more efficient penetration and dispersion of Al and Zr into the leather. They are accounted for by a more operative coordination ability and masking performance of the oligosaccharides. As such, the presence of oligosaccharides with abundant functional groups acts as an efficient 'Trojan horse' carrier, and all these phenomena are responsible for the high  $T_s$  (90.6 °C) of the tanned leather.

### Theoretical process optimization: toward a commercial tanning agent

Optimum conditions were sought for the selective conversion of hemicellulose in corncob into an advanced leather tanning material, making use of the empirical models developed. Due to the high predicted  $R^2$  attained for all the models (>0.95), they could be used for prediction purposes within the interval of variation considered in this work (Table 3). The optimization aims to maximize the hemicellulose conversion as well as minimize the cellulose and lignin conversion to achieve a very selective conversion of hemicellulose to produce xylo-oligomers. Also, to obtain a satisfactory tanning agent, it minimizes the chromaticity of the liquid fraction (hydrolysate) and maximizes the  $T_s$  of the tanned leather. To achieve this goal, optimum values for all the response variables were sought by assigning a relative importance (from 1 to 5) to each of the objectives to develop a solution that satisfies all the criteria.

Considering these conditions, the process is optimized using a catalytic synthesis system consisting of 56 mM  $AlCl_3$  and 2.6 vol%  $H_2O_2$  at 129 °C for 30 min. Under such conditions, 71.6% of hemicellulose in corncob was converted, while the conversion of cellulose and lignin was only 14.5% and 22.8%, respectively. The chromaticity of the obtained liquid fraction is 4405, while the  $T_s$  of the tanned leather is as high as 86.5 °C, much higher than the  $T_s$  (58.9 °C) of the

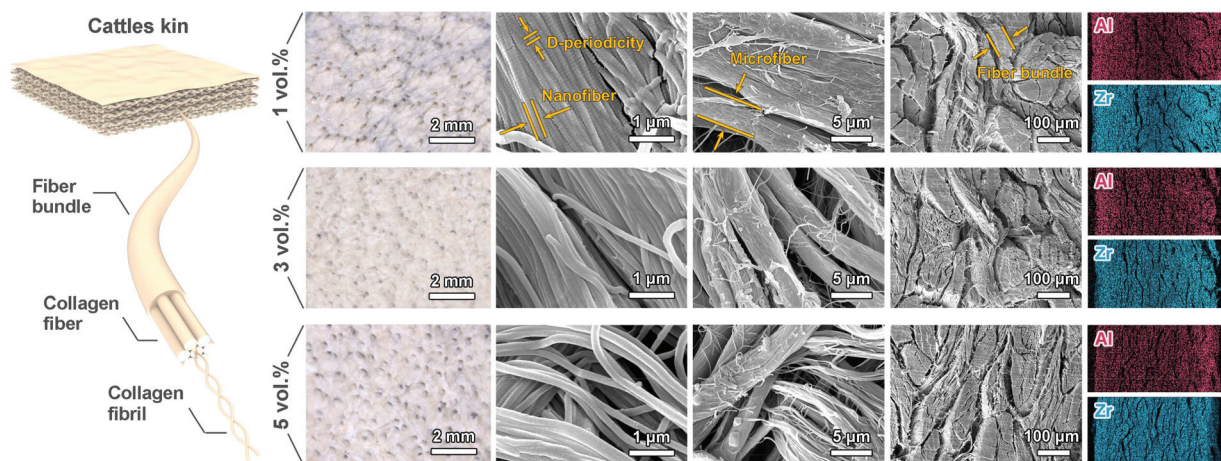


Fig. 8 Stereomicroscope images of the grain surface. SEM and Al/Zr EDS mapping images of the cross-section.



**Table 3** Theoretical optimization: operating conditions and response variables, including objectives, the interval of variation, relative importance, and theoretical and experimental optimum values

Variables	Objective	Interval of variation	Relative importance (1–5)	Optimum theoretical values
Temperature (°C)	None	100–160		129
AlCl <sub>3</sub> (mM)	None	10–100		56
H <sub>2</sub> O <sub>2</sub> (vol%)	None	1–5		2.6
C-Hemicellulose (%)	Maximize	0–100	5	71.6
C-Cellulose (%)	Minimize	0–100	3	14.5
C-Lignin (%)	Minimize	0–100	3	22.8
Chromaticity	Minimize	0–10 000	2	4405
T <sub>s</sub> (°C)	Maximize	0–100	5	86.5

untanned leather. The tear strength, tensile strength and softness of the leather tanned with our 'Al-Zr-oligosaccharide' tanning agent synthesized under optimum conditions were measured in duplicate. To gain more insights into our Trojan horse strategy, the original material was also tanned with the same amounts of Al and Zr in the absence of oligosaccharides ('Al-Zr'). Non-significant differences were observed in the mechanical strength obtained with the 'Al-Zr-oligosaccharide' and 'Al-Zr' tanning agents. The tear and tensile strengths were 13.5 N mm<sup>-2</sup> and 49.8 N mm<sup>-1</sup>, respectively, regardless of the tanning agent. Conversely, the softness of the tanned leather was higher with the 'Al-Zr-oligosaccharide' (8.6 mm) than with the 'Al-Zr' (7.1 mm) tanning agent. This difference is accounted for by the uniform penetration of Al and Zr achieved by using oligosaccharides as the carrier for our Trojan horse strategy, thus endowing the leather with excellent organoleptic properties. These conditions meet the very restrictive requirements of the wet white leather manufacturing industry, thus representing a landmark achievement towards the development of hazardous metal-free, environmentally friendly and highly efficient tanning agents from biomass.

## Conclusions

This work has explored the development of a pioneering 'advanced Trojan horse' strategy for the production of a tanning agent, based on 'Al-Zr-oligosaccharides' produced from corncob. As a first step, a microwave-assisted AlCl<sub>3</sub>-H<sub>2</sub>O<sub>2</sub>-H<sub>2</sub>O reaction system was used for the selective and simultaneous degradation and oxidation of hemicellulose in corncob, producing an aqueous solution containing 'Al-oligosaccharides' with abundant -CHO/-COOH functionalities. These oligosaccharides were then combined with Zr to produce 'Al-Zr-oligosaccharides' used for leather tanning. The effects of the reaction temperature (100–160 °C) and the AlCl<sub>3</sub> (10–100 mM) and H<sub>2</sub>O<sub>2</sub> (1–5 vol%) concentrations used in the synthesis step were systematically analyzed on the properties of the tanned leather. In this regard, the statistical analysis of the results revealed that the reaction temperature and the AlCl<sub>3</sub> concentration significantly influenced the hemicellulose

conversion. In contrast, the use of high H<sub>2</sub>O<sub>2</sub> concentrations increased the amounts of -CHO/-COOH functionalities in the oligosaccharides and strengthened their masking effect. As a result, the Al and Zr species were coordinated with these oligosaccharides and efficiently and uniformly penetrated the leather matrix (Trojan horse strategy) to crosslink with the collagen fibers. However, the temperature and the H<sub>2</sub>O<sub>2</sub> concentration must be carefully controlled. On the one side, high H<sub>2</sub>O<sub>2</sub> concentrations also destroyed the structures of lignin and crystalline cellulose, thus increasing the concentration of these species in the tanning liquid. On the other side, high reaction temperatures also promoted the generation of furans, which colored the aqueous solution containing the tanning agent, and led to color staining during the leather tanning process. Given these antagonistic effects, the optimization of the process revealed that using a temperature of 129 °C with an AlCl<sub>3</sub> concentration of 56 mM and a relative amount of H<sub>2</sub>O<sub>2</sub> of 2.6 vol% in the synthesis step, it is possible to convert up to 72 wt% of the hemicellulose present in corncob into an 'advanced Trojan horse' tanning agent. The use of this agent during the tanning of pickled cattle pelt produced a tanned material with a shrinkage temperature (T<sub>s</sub>) as high as 87 °C, thus meeting the restrictive requirements of the tanning industry. It could be used in the manufacture of different leathery materials, such as clothing, footwear, luggage and furnishing. Therefore, these results are a landmark achievement for leather manufacturing, thus allowing the development of a sustainable, chrome-free and eco-friendly leather industry.

## Experimental

### Materials

Corn cob powder was purchased from a local company, and it was washed with deionized water and dried at 105 °C in an oven for three days before use. AlCl<sub>3</sub>·6H<sub>2</sub>O, 30% H<sub>2</sub>O<sub>2</sub>, Zr(SO<sub>4</sub>)<sub>2</sub>·4H<sub>2</sub>O, NaCl and all the chemicals employed for the chemical titration were purchased from Sigma-Aldrich and Aladdin and used as received.

### Simultaneous degradation and oxidation of hemicellulose in corncob

The experiments for the production of the advanced tanning agent (synthesis step) were carried out in an Anton Paar microwave system, using 4 reactors per run. For each reaction, 10 g of corncob and 200 mL of deionized water, with varying concentrations of AlCl<sub>3</sub>·6H<sub>2</sub>O (0.01–0.1 mM) and H<sub>2</sub>O<sub>2</sub> (1–5 vol%, containing a Cu-Fe catalyst), were loaded into each of the four microwave Teflon tubes. The reactors were subsequently heated, and the reaction temperature was monitored inside the reaction tube using a ruby probe. Each reaction was heated from room temperature to the desired temperature (100–160 °C) within 4 min, and held for a reaction time of 30 min. After the treatment, the reaction system was cooled down to a temperature below 50 °C using compressed air. The post-treatment slurry was filtered to separate the solid residue





from the liquid fraction. The collected solid residue was dried overnight in an oven at 105 °C to calculate the overall conversion and stored for further analysis.

### Tanning process

Pickled cattle pelt was tailored along the backbone into matched pieces and weighed for the tanning process. The advanced tanning agent was produced from the hydrolysate (aqueous solution containing 'Al-oligosaccharide' complexes), with the addition of  $\text{AlCl}_3 \cdot 6\text{H}_2\text{O}$  (totally equal to 1 wt% of  $\text{Al}_2\text{O}_3$ ) along with  $\text{Zr}(\text{SO}_4)_2 \cdot 4\text{H}_2\text{O}$  (equal to 3 wt% of  $\text{ZrO}_2$ ) and 6 wt% of NaCl. Then, the pickled cattle skin and the tanning agent were added into a drum at a ratio of 2 : 1. The drum was then rotated at room temperature for 4 h. After this, in the second step, the pH of the tanning liquor was progressively adjusted to *ca.* 4.0 with a sodium bicarbonate solution at an interval of 5 min. The third step is the tanning process itself, wherein the drum was run for 4 h at 40 °C and then stood for 12 h to achieve a complete crosslinking reaction between the advanced tanning agent and the collagen fibers. Finally, the tanned leather produced was washed with deionized water at room temperature for 1 min, and then dried with air for further characterization and evaluation.

### Experimental design and data analysis

The influence of the reaction temperature (100–160 °C), and the  $\text{AlCl}_3$  (0.01–0.1 mM) and  $\text{H}_2\text{O}_2$  (1–5 vol%) concentrations during the conversion of corncob (synthesis step) was investigated for the production of the 'advanced Trojan horse' tanning agent. According to a 2 level 3 factor Box–Wilson central composite face centred (CCF,  $\alpha$ :  $\pm 1$ ) design, the experiments were planned. This involves a  $2^3$  factorial design, which represents the number of runs for the simple factorial design, along with 8 additional axial experiments to study the non-linear effects and interactions, and 3 replicates at the center of the variation interval of each factor were carried out to evaluate the experimental error. This experimental series is sufficient to investigate the influence of each variable (linear and quadratic effects) together with all the possible interactions between them. All the results were studied by one-way analysis of variance (ANOVA) with 95% confidence. Moreover, the cause–effect Pareto principle was adopted to calculate the relative importance of the operating variables and interactions on the response variables. To estimate the effects of all operating variable factors in equal terms, the lower and upper limits were normalized within the same interval (from –1 to 1). The ANOVA was conducted with 95% confidence ( $p$ -value = 0.05). For the models developed, the lack of fit was not significant with 95% confidence ( $p$ -value > 0.05). This information has been included in the revised version of the manuscript.

### Response variables and analytical methods

Several response variables were employed to analyze the effects of using biomass as a tanning carrier during the preparation of the 'Al–Zr-oligosaccharide' water solution. These include the response variables related to (i) the first conversion of

biomass to produce the tanning agent: the conversion of the three main components (hemicellulose, cellulose and lignin) in corncob and the chemical composition (yields of monosaccharides, carboxylic acids and furans) and chromaticity of the hydrolysate; and (ii) the performance of the tanning agent produced from the liquid (hydrolysate) obtained in the first step: the tanned leather shrinkage temperature ( $T_s$ ), along with the Al and Zr absorptions on this product.

To calculate the conversion of hemicellulose, cellulose and lignin, the contents of these three main components were quantitatively analyzed by chemical titration according to our previous work.<sup>27,31</sup> The chemical composition of the hydrolysate (amounts of monosaccharides, carboxylic acids and furans) was analyzed using a 1260 Infinity II Agilent HPLC equipped with a RI detector and an Aminex HPX-87H column (300 mm  $\times$  7.8 mm, Bio-Rad). A 5 mmol L<sup>–1</sup>  $\text{H}_2\text{SO}_4$  solution was used as the mobile phase at a flow rate of 0.6 mL min<sup>–1</sup>. The chromaticity of the hydrolysate was measured by Lovibond (EC 2000-Pt–Co) using the platinum–cobalt method, and deionized water was used as a blank test.

After the tanning process, the temperature of the tanned leather  $T_s$  was measured and recorded using a digital leather shrinkage temperature instrument (MSW-YD4, Shaanxi University of Science and Technology) at a heating rate of 2 °C min<sup>–1</sup>, testing each sample in triplicate. The grain surface of the tanned leather was observed using a stereomicroscope (SZX12, Olympus). After a freeze-drying step, to remove the moisture from the leather, the cross-section of the tanned leather was observed using a scanning electron microscope (SEM, JSM-7500F, JEOL), equipped with an energy-dispersive spectroscopy (EDS) analyzer. To evaluate the absorption rate of Al and Zr into/onto the leather, the residual contents of Al and Zr in the liquid post-tanning agent were determined by ICP-OES.

## Conflicts of interest

There are no conflicts to declare.

## Acknowledgements

This work is financially supported by the National Natural Science Foundation of China (22078211), the China Postdoctoral Science Foundation (2019M663489), the Sichuan Science and Technology Program (2020YJ0023) and the Fundamental Research Funds for the Central Universities (2019SCU12059). We appreciate Hui Wang from the Analytical & Testing Center of Sichuan University for help with SEM characterization. We also thank Dr Xiu He at the College of Biomass Science and Engineering, Sichuan University, for experimental assistance. Besides, Javier Remón is very grateful to the Spanish Ministry of Science, Innovation and Universities for the Juan de la Cierva (JdC) fellowship (IJC2018-037110-I) awarded. We acknowledge support of the publication fee by the CSIC Open Access Publication Support Initiative through its Unit of Information Resources for Research (URICI).



## References

- 1 X. Wang, K. Gao, X. Ye, X. Huang and B. Shi, *Chem. Eng. J.*, 2018, **344**, 625–632.
- 2 X. Huang, X. Kong, Y. Cui, X. Ye, X. Wang and B. Shi, *Chem. Eng. J.*, 2018, **336**, 633–639.
- 3 W. Ding, X. Pang, Z. Ding, D. C. W. Tsang, Z. Jiang and B. Shi, *J. Hazard. Mater.*, 2020, **396**, 122771.
- 4 Y. Yi, Z. Jiang, S. Yang, W. Ding, Y. Wang and B. Shi, *Carbohydr. Polym.*, 2020, **239**, 116217.
- 5 Y. S. Hedberg, *J. Leather Sci. Eng.*, 2020, **2**, 20.
- 6 W. Huang, Y. Song, Y. Yu, Y. Wang and B. Shi, *J. Leather Sci. Eng.*, 2020, **2**, 8.
- 7 B. Wu, S. Yu, G. Zhang, S. Zhang, P. Shen and P. G. Tratnyek, *J. Hazard. Mater.*, 2020, **400**, 123306.
- 8 B. Li, P. Liao, L. Xie, Q. Li, C. Pan, Z. Ning and C. Liu, *Water Res.*, 2020, **181**, 115923.
- 9 Y. Yu, Y. Wang, W. Ding, J. Zhou and B. Shi, *Carbohydr. Polym.*, 2017, **174**, 823–829.
- 10 M. Sathish, B. Madhan, K. J. Sreeram, J. Raghava Rao and B. U. Nair, *J. Cleaner Prod.*, 2016, **112**, 49–58.
- 11 B. Madhan, A. Sundarrajan, J. R. Rao and B. U. Nair, *J. Am. Leather Chem. Assoc.*, 2003, **98**, 107–114.
- 12 K. J. Sreeram, M. Kanthimathi, J. Raghava Rao, R. Sundaram and T. Ramasami, *J. Am. Leather Chem. Assoc.*, 2000, **95**, 324–332.
- 13 B. Wang, Y. Sun and R. Sun, *J. Leather Sci. Eng.*, 2019, **1**, 5.
- 14 J. Remón, M. Casales, J. Gracia, M. S. Callén, J. L. Pinilla and I. Suelves, *Chem. Eng. J.*, 2021, **405**, 126705.
- 15 Z. Jiang, P. Zhao and C. Hu, *Bioresour. Technol.*, 2018, **256**, 466–477.
- 16 Z. Jiang, W. Ding, S. Xu, J. Remón, B. Shi, C. Hu and J. H. Clark, *Green Chem.*, 2020, **22**, 316–321.
- 17 Z. Jiang, J. Fan, V. L. Budarin, D. J. Macquarrie, Y. Gao, T. Li, C. Hu and J. H. Clark, *Sustainable Energy Fuels*, 2018, **2**, 936–940.
- 18 J. Fan, M. De bruyn, V. L. Budarin, M. J. Gronnow, P. S. Shuttleworth, S. Breeden, D. J. Macquarrie and J. H. Clark, *J. Am. Chem. Soc.*, 2013, **135**, 11728–11731.
- 19 J. Li, Z. Jiang, L. Hu and C. Hu, *ChemSusChem*, 2014, **7**, 2482–2488.
- 20 J. Yi, T. He, Z. Jiang, J. Li and C. Hu, *Chin. J. Catal.*, 2013, **34**, 2146–2152.
- 21 Z. Jiang, V. L. Budarin, J. Fan, J. Remón, T. Li, C. Hu and J. H. Clark, *ACS Sustainable Chem. Eng.*, 2018, **6**, 4098–4104.
- 22 Q. Li, A. Wang, K. Long, Z. He and R. Cha, *ACS Sustainable Chem. Eng.*, 2018, **7**, 1129–1136.
- 23 Y. Xie, X. Wang, W. Tong, W. Hu, P. Li, L. Dai, Y. Wang and Y. Zhang, *Chem. Eng. J.*, 2020, **396**, 125321.
- 24 Z. Jiang, J. Yi, J. Li, T. He and C. Hu, *ChemSusChem*, 2015, **8**, 1901–1907.
- 25 Z. Jiang, P. Zhao, J. Li, X. Liu and C. Hu, *ChemSusChem*, 2018, **11**, 397–405.
- 26 L. Shuai and J. Luterbacher, *ChemSusChem*, 2016, **9**, 133–155.
- 27 Z. Jiang, T. He, J. Li and C. Hu, *Green Chem.*, 2014, **16**, 4257–4265.
- 28 Z. Jiang and C. Hu, *J. Energy Chem.*, 2016, **25**, 947–956.
- 29 X. Fu, J. Dai, X. Guo, J. Tang, L. Zhu and C. Hu, *Green Chem.*, 2017, **19**, 3334–3343.
- 30 H. Xu, Y. Wang, X. Liao and B. Shi, *J. Energy Chem.*, 2020, **47**, 324–332.
- 31 L. Hu, Y. Luo, B. Cai, J. Li, D. Tong and C. Hu, *Green Chem.*, 2014, **16**, 3107–3116.

